

A porous metal–metalloporphyrin framework featuring high-density active sites for chemical fixation of CO₂ under ambient conditions†

Cite this: *Chem. Commun.*, 2014, 50, 5316Received 1st October 2013,
Accepted 5th November 2013

DOI: 10.1039/c3cc47542e

www.rsc.org/chemcomm

Wen-Yang Gao, Lukasz Wojtas and Shengqian Ma*

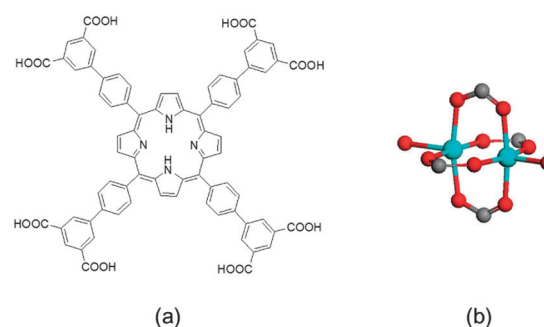
Self-assembly of the custom-designed octatopic porphyrin ligand of tetrakis(3,5-dicarboxyphenyl)porphine with the *in situ* generated Cu₂(CO₂)₄ paddlewheel moieties afforded a porous metal–metalloporphyrin framework, MMPF-9, which features a high density of Cu(II) sites confined within nanoscopic channels and demonstrates excellent performances as a heterogeneous Lewis-acid catalyst for chemical fixation of CO₂ to form carbonates at room temperature under 1 atm pressure.

Metal–organic frameworks (MOFs),¹ which consist of metal ions or metal clusters (also known as secondary building units, SBUs)² that are interconnected by multitopic organic ligands to form two- or three-dimensional (2D or 3D) networks, have been expanding at a rapid pace over the past decade. A major driving force behind their surge lies in their amenability to design: a desired structure can thus be targeted by judicious selection of the SBU and the organic linker.³ Furthermore, their modular nature means that their properties (for example, pore sizes, pore walls and surface area) can also be tailored or tuned by custom design of organic linkers.⁴ Driven by the motivation to mimic ubiquitous biological functions of metalloporphyrins in nature, such as light-harvesting, oxygen transportation and catalysis,⁵ porphyrin/metalloporphyrin-based linkers are of increasing interest for incorporation into MOF frameworks to afford porphyrin-based MOFs.⁶ Indeed, porphyrin-based MOFs have exhibited potential for applications in gas storage/separation,⁷ light-harvesting,⁸ catalysis⁹ and other areas,¹⁰ as recently demonstrated by our group and others.^{6–10}

During the course of constructing porphyrin-based MOFs, the porphyrin macrocycles of the linkers could be metallated *in situ* with the same metal ions as those in the SBUs.^{6a–d,10a,b} This represents an appealing approach to create a high density of

metal sites into 3D nanospace, which could be particularly tempting for catalysis if the metal centers both within the porphyrin rings and on the SBUs are catalytically active.^{6d,f} In this contribution, we report such a porphyrin-based MOF, MMPF-9 (MMPF denotes metal–metalloporphyrin framework), the channelled structure of which is sustained by the Cu(II) *in situ* metallated porphyrin ligands of tetrakis(3,5-dicarboxyphenyl)porphine (tdcbpp, Scheme 1a) and the copper paddlewheel SBUs (Scheme 1b). MMPF-9 thus features a high density of Cu(II) sites in the confined nanospace, proving it to be a highly efficient Lewis-acid heterogeneous catalyst for chemical fixation of CO₂ to form cyclic carbonates at room temperature under 1 atm pressure.

The dark red block-shaped crystals of MMPF-9 were harvested by reacting H₁₀tdcbpp with Cu(NO₃)₂·2.5H₂O under solvothermal conditions. Single-crystal X-ray diffraction analysis revealed that MMPF-9 crystallizes in the hexagonal space group *P6₃/mmc* with an empirical formula Cu₆(CuC₇₆H₃₆N₄O₁₆)(HCO₂)₄(H₂O)₆.† There exist two types of copper paddlewheel units in MMPF-9. The first type is those bridged by four carboxylate groups of four different tdcbpp ligands with two aqua ligands at the axial positions. The second type is those consisting of two coplanar carboxylate groups of two different tdcbpp ligands; two coplanar coordinated formate ions and two axial coordinated water molecules (Fig. S1, ESI†). The first type copper paddlewheel units can be simplified as 4-connected



Scheme 1 (a) Tetrakis(3,5-dicarboxyphenyl)porphine (H₁₀tdcbpp) ligand; (b) the copper paddlewheel SBU (gray, C; red, O; turquoise, Cu).

Department of Chemistry, University of South Florida, 4202 East Flower Avenue, Tampa, Florida 33620, USA. E-mail: sqma@usf.edu; Fax: +1-813-974 3203; Tel: +1-813-974 5217

† Electronic supplementary information (ESI) available: Experimental details, N₂ adsorption isotherms, topological pictures, TGA plots and single-crystal data. CCDC 961077. For ESI and crystallographic data in CIF or other electronic format see DOI: 10.1039/c3cc47542e

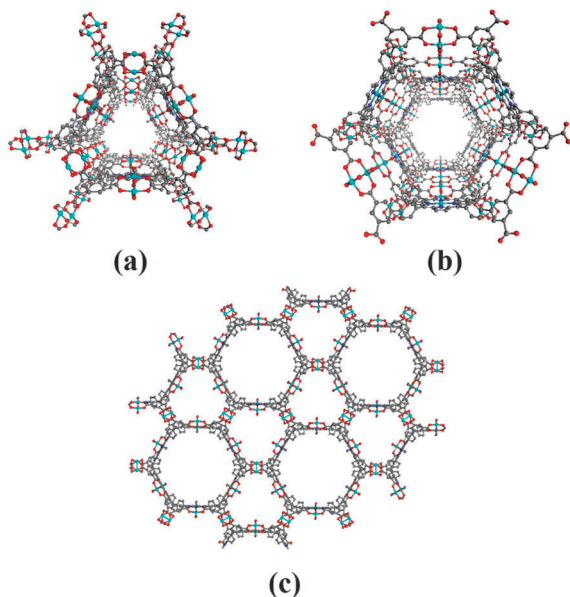


Fig. 1 (a) The truncated triangular channel, (b) the hexagonal channel, and (c) the extended channels of MMPF-9 viewed along the *c* direction.

nodes whereas the second type can be considered as ditopic bridges. The porphyrin macrocycles of tdcbpp ligands are *in situ* metallated with Cu(II) during the synthesis process. Each Cu(II)-metallated tdcbpp [hereafter tdcbpp(Cu)] ligand connects eight SBUs through carboxylate groups of four isophthalate moieties to extend into a 3D framework. Two types of channels, truncated triangular (Fig. 1a) and hexagonal (Fig. 1b), are observed along the *c* direction. The truncated triangular channel with an edge of ~ 14.0 Å (atom to atom distance) is enclosed by three tdcbpp(Cu) ligands that are linked together through six 4-connected copper paddlewheel units (Fig. S2, ESI[†]). This means that an array of nine copper sites point toward the truncated triangular channel. The hexagonal channel is formed by three tdcbpp(Cu) ligands that are bridged by six 2-connected copper paddlewheel units (Fig. S3, ESI[†]), and has an aperture of 24.7 Å (atom to atom distance) along the diagonal. The hexagonal channel also features an array of nine copper sites that orient toward the channel center. Topologically, MMPF-9 possesses a rare (4,12)-connected dinodal net (Fig. S5, ESI[†]) with a new topology of *smv* (point symbol: $(3^{16}\cdot 4^{24}\cdot 5^{20}\cdot 6^6)(3^4\cdot 4^2)$) if the first type copper paddlewheel units are simplified as 4-connected nodes and the basic building blocks (three tdcbpp(Cu) ligands linked to six second type copper paddlewheel units through 12 carboxyl groups) forming the hexagonal channel are considered as 12-connected nodes. MMPF-9 is porous and has a solvent accessible volume of 80.0% as calculated using PLATON.¹¹

The phase purity of MMPF-9 was verified by powder X-ray diffraction (PXRD) studies, which indicate that the diffraction patterns of the fresh sample are consistent with the calculated ones (Fig. S6, ESI[†]). To assess the permanent porosity of MMPF-9, an N_2 adsorption isotherm at 77 K was measured for the activated sample, which reveals an uptake capacity of ~ 245 cm³ g⁻¹ at the saturation pressure with typical type I adsorption behaviour (Fig. S8, ESI[†]), a characteristic of microporous materials. Derived from the N_2 adsorption data, MMPF-9 possesses a Brunauer–Emmett–Teller

(BET) surface area of ~ 850 m² g⁻¹ ($P/P_0 = 0.0001$ – 0.1) corresponding to a Langmuir surface area of 1050 m² g⁻¹ ($P/P_0 = 0.9$).

MOFs have recently been demonstrated to serve as heterogeneous Lewis acid catalysts for chemical conversion of CO₂ into cyclic carbonates but under the conditions of high pressure (>3 MPa) and high temperature (>100 °C).¹² Given the high density of copper sites confined within the nanoscopic channels of MMPF-9, we decided to evaluate its performances as a Lewis acid catalyst in the context of cycloaddition of CO₂ and epoxides to form cyclic carbonates at room temperature under 1 atm pressure. As shown in Table 1, MMPF-9 demonstrates highly efficient catalytic activity for cycloaddition of propylene oxide using CO₂ to form propylene carbonate at room temperature under 1 atm CO₂ pressure with a yield of 87.4% over 48 hours (Table 1, entry 1). MMPF-9 outperforms the benchmark copper MOF of HKUST-1, which exhibits a moderate activity to form propylene carbonate in 49.2% yield over 48 h under similar reaction conditions (Table 1, entry 2). We reasoned that the high catalytic activity of MMPF-9 for chemical fixation of CO₂ under ambient conditions should be mainly ascribed to the high density of active sites confined in the accessible nanoscopic channels.

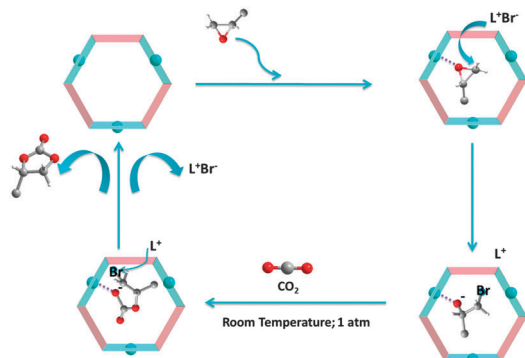
We examined the performances of MMPF-9 in chemical fixation of CO₂ with different functional group substituted epoxides under the ambient conditions. A high catalytic activity was also observed for cycloaddition of butylene oxide using CO₂ to form butylene carbonate at room temperature under 1 atm pressure with a yield of 80.3% over 48 hours (Table 1, entry 3). Interestingly, with the increase of molecular sizes of epoxide substrates, a substantial decrease in the yield of cyclic carbonate was

Table 1 Different substituted epoxides coupled with CO₂ catalyzed by MOFs at room temperature under 1 atm pressure

Entry	Epoxides	Products	Yield (%)
1 ^a			87.4
2 ^b			49.2
3 ^a			80.3
4 ^a			30.5
5 ^c			65.9
6 ^a			29.7
7 ^d			86.4

^a Reaction conditions: epoxide (25 mmol) with MMPF-9 (0.03125 mmol), *n*-Bu₄NBr (0.58 g), at room temperature under 1 atm CO₂ for 48 hours.

^b The same reaction conditions as those when loaded with HKUST-1 (0.03125 mmol). ^c Reaction time was extended to 96 hours under the similar conditions. ^d The recyclability test of MMPF-9.



Scheme 2 The schematic representation of the tentatively proposed catalytic mechanism for the cycloaddition of epoxides and CO₂ into cyclic carbonates catalyzed by MMPF-9 (turquoise ball: Cu(II) site from either the porphyrin center or copper paddlewheel units).

observed, as indicated by the 30.5% yield of 3-butoxy-1,2-propylene carbonate (Table 1, entry 4) and 29.7% yield of 3-allyloxy-1,2-propylene carbonate (Table 1, entry 5) from butyl glycidyl ether and allyl glycidyl ether, respectively. This could be attributed to the limited diffusion of large-sized epoxide molecules thus displaying “apparent” size-selective catalysis.¹³ Nonetheless, the yield of cyclic carbonate increases from 30.5% to 65.9% (Table 1, entry 5) for butyl glycidyl ether when the reaction time is extended from 48 hours to 96 hours, which can be tentatively ascribed to the heavily delayed mass transportation for large-sized substitute molecules. MMPF-9 can be recycled without significant drop in catalytic activity (Table 1, entry 6).

According to some literatures,¹² a tentative mechanism was proposed for the cycloaddition of epoxides and CO₂ to form cyclic carbonate catalyzed by MMPF-9, as illustrated in Scheme 2. The epoxide first binds with the Lewis acidic copper site in the nanoscopic channel of MMPF-9 through the oxygen atom of epoxide, and this step leads to the activation of the epoxy ring. The less-hindered carbon atom of the activated epoxide is then attacked by the Br⁻ generated from *n*-Bu₄NBr to open the epoxy ring. Subsequently CO₂ interacts with the oxygen anion of the opened epoxy ring to form an alkylcarbonate anion, which is then converted into the corresponding cyclic carbonate through a ring closing step. We speculate that a high density of copper Lewis acid sites pointing toward the channel center could boost the synergistic effect using *n*-Bu₄NBr thus facilitating the cycloaddition reaction, which thereby results in high catalytic activity of MMPF-9 for converting CO₂ into cyclic carbonates under ambient conditions. Notwithstanding, detailed mechanistic studies to probe the intermediates during the cycloaddition reaction could be necessary, and research along this line will be conducted in the near future.

In summary, a porous metal-metalloporphyrin framework, MMPF-9, was constructed using a custom-designed octatopic porphyrin ligand that links Cu₂(CO₂)₄ paddlewheel moieties. MMPF-9 features a high density of copper sites in the nanoscopic channels, proving it to be a highly efficient Lewis acid-based heterogeneous catalyst for chemical fixation of CO₂ with epoxides to form cyclic carbonates under ambient conditions. Ongoing work in our laboratory includes the construction of

new MOF-based heterogeneous catalysts for chemical fixation of CO₂ and the development of new MMPFs for applications in heterogeneous catalysis.

The authors acknowledge the University of South Florida for financial support of this work.

Notes and references

‡ X-ray crystal data for MMPF-9: C₈₀H₄₀N₄O₃₀Cu₇, *f*_w = 1981.94, hexagonal, *P*6₃/*mmc*, *a* = 33.7831(10) Å, *b* = 33.7831(10) Å, *c* = 43.456(3) Å, *V* = 42952 (3) Å³, *Z* = 6, *T* = 228(2) K, ρ_{calcd} = 0.460 g cm⁻³, *R*₁ (*I* > 2σ(*I*)) = 0.0485, w*R*₂ (all data) = 0.1354, CCDC 961077.

- H.-C. Zhou, J. R. Long and O. M. Yaghi, *Chem. Rev.*, 2012, **112**, 673.
- (a) B. Moulton and M. J. Zaworotko, *Chem. Rev.*, 2001, **101**, 1629; (b) M. O’Keeffe and O. M. Yaghi, *Chem. Rev.*, 2012, **112**, 675.
- (a) S. Kitagawa, R. Kitaura and S.-I. Noro, *Angew. Chem., Int. Ed.*, 2004, **43**, 2334; (b) S. Qiu and G. Zhu, *Coord. Chem. Rev.*, 2009, **253**, 2891.
- (a) O. M. Yaghi, M. O’Keeffe, N. W. Ockwig, H. K. Chae, M. Eddaoudi and J. Kim, *Nature*, 2003, **423**, 705; (b) M. O’Keeffe, *Chem. Soc. Rev.*, 2009, **38**, 1215.
- (a) J. Barber and B. Andersson, *Nature*, 1994, **370**, 31; (b) G. McDermott, S. M. Prince, A. A. Freer, A. M. Hawthornthwaite-Lawless, M. Z. Papiz, R. J. Cogdell and N. W. Isaacs, *Nature*, 1995, **374**, 517; (c) Y.-C. Cheng and G. R. Fleming, *Annu. Rev. Phys. Chem.*, 2009, **60**, 241.
- (a) X.-S. Wang, L. Meng, Q. Cheng, C. Kim, L. Wojtas, M. Chrzanowski, Y.-S. Chen, X. P. Zhang and S. Ma, *J. Am. Chem. Soc.*, 2011, **133**, 16322; (b) X.-S. Wang, M. Chrzanowski, C. Kim, W.-Y. Gao, L. Wojtas, Y.-S. Chen, X. P. Zhang and S. Ma, *Chem. Commun.*, 2012, **48**, 7173; (c) X.-S. Wang, M. Chrzanowski, W.-Y. Gao, L. Wojtas, Y.-S. Chen, M. J. Zaworotko and S. Ma, *Chem. Sci.*, 2012, **3**, 2823; (d) L. Meng, Q. Cheng, C. Kim, W.-Y. Gao, L. Wojtas, Y.-S. Chen, M. J. Zaworotko, X. P. Zhang and S. Ma, *Angew. Chem., Int. Ed.*, 2012, **51**, 10082; (e) Y. Chen, T. Hoang and S. Ma, *Inorg. Chem.*, 2012, **51**, 12600; (f) X.-S. Wang, M. Chrzanowski, L. Wojtas, Y.-S. Chen and S. Ma, *Chem.-Eur. J.*, 2013, **19**, 3297; (g) W.-Y. Gao, Z. Zhang, L. Cash, L. Wojtas, Y.-S. Chen and S. Ma, *CrystEngComm*, 2013, **15**, 9320.
- (a) W. Morris, B. Voloskiy, S. Demir, F. Gandara, P. L. McGrier, H. Furukawa, D. Cascio, J. F. Stoddart and O. M. Yaghi, *Inorg. Chem.*, 2012, **51**, 6443; (b) J. A. Johnson, Q. Lin, L.-C. Wu, N. Obaidi, Z. L. Olson, T. C. Reeson, Y.-S. Chen and J. Zhang, *Chem. Commun.*, 2013, **49**, 2828.
- (a) C. Y. Lee, O. K. Farha, B. J. Hong, A. A. Sarjeant, S. T. Nguyen and J. T. Hupp, *J. Am. Chem. Soc.*, 2011, **133**, 15858; (b) H.-J. Son, S. Jin, S. Patwardhan, S. J. Wezenberg, N. C. Jeong, M. So, C. E. Wilmer, A. A. Sarjeant, G. C. Schatz, R. Q. Snurr, O. K. Farha, G. P. Wiederrecht and J. T. Hupp, *J. Am. Chem. Soc.*, 2013, **135**, 862.
- (a) O. K. Farha, A. M. Shultz, A. A. Sarjeant, S. T. Nguyen and J. T. Hupp, *J. Am. Chem. Soc.*, 2011, **133**, 5652; (b) A. Fateeva, P. A. Chater, C. P. Ireland, A. A. Tahir, Y. Z. Khimyak, P. V. Wiper, J. R. Darwent and M. J. Rosseinsky, *Angew. Chem., Int. Ed.*, 2012, **51**, 7440; (c) D. Feng, Z.-Y. Gu, J.-R. Li, H.-L. Jiang, Z. Wei and H.-C. Zhou, *Angew. Chem., Int. Ed.*, 2012, **51**, 10307; (d) C. Zou, Z. Zhang, X. Xu, Q. Gong, J. Li and C.-D. Wu, *J. Am. Chem. Soc.*, 2012, **134**, 87.
- (a) M. E. Kosal, J. H. Chou, S. R. Wilson and K. S. Suslick, *Nat. Mater.*, 2002, **1**, 118; (b) I. Goldberg, *Chem. Commun.*, 2005, 1243; (c) B. J. Burnett, P. M. Barron, C. Hu and W. Choe, *J. Am. Chem. Soc.*, 2011, **133**, 9984; (d) S. Motoyama, R. Makiura, O. Sakata and H. Kitagawa, *J. Am. Chem. Soc.*, 2011, **133**, 5460; (e) M. Jahan, Q. Bao and K. P. Loh, *J. Am. Chem. Soc.*, 2012, **134**, 6707.
- A. L. Spek, *J. Appl. Crystallogr.*, 2003, **36**, 7.
- (a) J. Song, Z. Zhang, S. Hu, T. Wu, T. Jiang and B. Han, *Green Chem.*, 2009, **11**, 1031; (b) E. E. Macias, P. Ratnasamy and M. A. Carreon, *Catal. Today*, 2012, **198**, 215; (c) C. M. Miralda, E. E. Macias, M. Zhu, P. Ratnasamy and M. A. Carreon, *ACS Catal.*, 2012, **2**, 180; (d) J. Kim, S.-N. Kim, H.-G. Jang, G. Seo and W.-S. Ahn, *Appl. Catal., A*, 2013, **453**, 175; (e) M. Zhu, D. Srinivas, S. Bhogeswararao, P. Ratnasamy and M. A. Carreon, *Catal. Commun.*, 2013, **32**, 36.
- (a) S. Horike, M. Dincă, K. Tamaki and J. R. Long, *J. Am. Chem. Soc.*, 2008, **130**, 5854; (b) A. Corma, H. Garcia and F. X. Llabres i Xamena, *Chem. Rev.*, 2010, **110**, 4606.